



**Environmental  
Science**  
Nano

**Urban runoff drives titanium dioxide engineered particle concentrations in urban watersheds: field measurements**

Journal:	<i>Environmental Science: Nano</i>
Manuscript ID	EN-ART-09-2022-000826.R2
Article Type:	Paper

**SCHOLARONE™**  
Manuscripts

## Environmental significance

Spatiotemporal monitoring of anthropogenic (engineered and incidental) metal-bearing nanoparticles in environmental systems is essential to improve the understanding of the nature, sources, magnitude of exposure, environmental fate, and risk assessment of these materials. Here we monitored - daily over 16 days - the concentrations of anthropogenic Ti-bearing particles in three rivers (Lower Saluda, Broad, and Congaree) within the urban outskirts of the City of Columbia, South Carolina, United States. The higher bulk Ti/Nb mass ratios than the natural background ratios and the similarity of natural the fingerprint of multi-element Ti-bearing to those of natural particles suggest that the samples are contaminated with single metal Ti-bearing particles which can be attributed to pure TiO<sub>2</sub> particles. The concentration of anthropogenic TiO<sub>2</sub> were minimal in the Lower Saluda River downstream Lake Murray reservoir and increased from the Broad to the Congaree River along the city of Columbia. The concentration of anthropogenic TiO<sub>2</sub> followed the same trend of increases and decreases as the discharge/runoff. Thus, anthropogenic TiO<sub>2</sub> particles were attributed to urban runoff from the City of Columbia. These findings suggest that aquatic organisms in urban waters within the outskirts and downstream of highly urbanized and mega cities are frequently exposed to transient high concentrations of anthropogenic TiO<sub>2</sub> particles, as well as other particles and contaminants carried with urban runoff.

1  
2  
3 **Urban runoff drives titanium dioxide engineered particle concentrations in**  
4  
5  
6 **urban watersheds: field measurements**  
7  
8  
9

10  
11 Md. Mahmudun Nabi<sup>1</sup>, Jingjing Wang<sup>a</sup>, Mahdi Erfani<sup>b</sup>, Erfan Goharian<sup>b</sup>, and Mohammed  
12  
13 Baalousha<sup>a\*</sup>  
14  
15

16  
17  
18  
19  
20 **Affiliations:**  
21

22  
23 <sup>a</sup> Center for Environmental Nanoscience and Risk, Department of Environmental Health Sciences,  
24  
25 Arnold School of Public Health, University of South Carolina, SC 29208, USA  
26

27  
28 <sup>b</sup> Department of Civil and Environmental Engineering, University of South Carolina, SC 29208,  
29  
30 USA  
31

32  
33  
34  
35 \* Corresponding author: [mbaalous@mailbox.sc.edu](mailto:mbaalous@mailbox.sc.edu)  
36  
37  
38  
39  
40  
41  
42  
43  
44  
45  
46  
47  
48  
49  
50  
51  
52  
53  
54  
55  
56  
57  
58  
59  
60

## Abstract

Urban runoff is a significant source of pollutants, including incidental and engineered nanoparticles, to receiving surface waters. The aim of this study is to investigate the impact of urbanization on the concentrations of TiO<sub>2</sub> engineered particles in urban surface waters. The study area boundaries are limited to the Lower Saluda and Nicholas Creek-Broad River from upstream, and outlet of upper Congaree River in Columbia, South Carolina, United States from downstream. This sampling area captures a significant footprint of the urban area of the City of Columbia. Water samples were collected daily from four sites during two rain events. All samples were analyzed for total metal concentrations following acid digestion and for particle number concentration and elemental composition using single particle-inductively coupled plasma-time of flight-mass spectrometry (SP-ICP-TOF-MS). The Ti/Nb ratios in the Broad and Congaree River samples are generally higher than those of natural background ratios, indicating contamination of these two rivers with anthropogenic Ti-bearing particles. Clustering of multi-metal nanoparticles (mmNPs) demonstrated that Ti-bearing particles are distributed mainly among three clusters, FeTiMn, AlSiFe, and TiMnFe, which are typical of naturally occurring iron oxide, clay, and titanium oxide particles, indicating the absence of significance of anthropogenic multi-element Ti-bearing particles. Thus, anthropogenic Ti-bearing particles are attributed to single-metal particles; that is pure TiO<sub>2</sub> particles. The total concentration of anthropogenic TiO<sub>2</sub> in the rivers was determined by mass balance calculation using bulk titanium concentration and increases in Ti/Nb above the natural background ratio. The concentration of anthropogenic TiO<sub>2</sub> increases following the order 0 to 24 μg L<sup>-1</sup> in the Lower Saluda River < 0 to 663 μg L<sup>-1</sup> in the Broad River < 43 to 1051 μg L<sup>-1</sup> in Congaree River at Cayce < 58 to 5050 μg L<sup>-1</sup> in the Congaree River at Columbia. The concentration of anthropogenic TiO<sub>2</sub> increases with increases in urban runoff. The source of anthropogenic TiO<sub>2</sub> is attributed to diffuse urban runoff. This study demonstrates that diffuse urban runoff results in high concentrations of TiO<sub>2</sub> particles in urban surface waters during and following rainfall events which may pose increased risks to aquatic organisms during these episodic events.

## 1. Introduction

Urban runoff is widely recognized as a major vector of pollutants, including engineered and incidental nanoparticles (ENPs and INPs), from the urban environment to receiving surface waters, contributing to the deterioration of urban surface water quality<sup>1</sup>. Yet, there is a limited understanding of the impacts of urbanization and urban runoff on the concentrations of engineered particles in urban surface waters<sup>2</sup>. Titanium dioxide (TiO<sub>2</sub>) is the most widely used engineered particles in the urban environment both as pigments (*e.g.*, 100-300 nm) in paint and as nanosized particles (*e.g.*, 1-100 nm) in self-cleaning surfaces such as photocatalysts<sup>3</sup>. For instance, an estimated 5.3 billion liters year<sup>-1</sup> paint were used in the United States in 2019, 33% of which (*e.g.*, 1.77 billion liters year<sup>-1</sup>) was used for exterior paint<sup>4</sup>. These uses of TiO<sub>2</sub> result in their release due to wear and tear into the atmosphere and deposition on urban surfaces<sup>5-9</sup>. Rainfall washes the atmospheric deposited particles and carries them into receiving waterbodies. Thus, TiO<sub>2</sub> engineered particles are expected to occur at high concentrations in urban surface waters.

Urban waters receive large amounts of pollution, including TiO<sub>2</sub> engineered particles, from a variety of sources such as industrial discharges, mobile sources (*e.g.*, cars and trucks), residential and commercial wastewater, and polluted stormwater runoff from urban landscape. Recent studies reported high concentrations of TiO<sub>2</sub> engineered particles in road dust (*e.g.*, 0.4-2.5 g·kg<sup>-1</sup>)<sup>10-16</sup>, bridge runoff (*e.g.*, 5-150 µg L<sup>-1</sup>)<sup>17-19</sup>, sanitary sewer overflow- impacted surface waters (*e.g.*, 1-100 µg L<sup>-1</sup>)<sup>20,21</sup>, urban runoff- impacted surface waters (*e.g.*, 20 to 140 µg L<sup>-1</sup>)<sup>22</sup>, and industrial discharge- impacted surface waters (*e.g.*, 133 to 266 µg L<sup>-1</sup>)<sup>23,24</sup>. Additionally, a recent modeling study predicted even higher concentrations TiO<sub>2</sub> ENPs (*e.g.*, 619 to 1490 µg L<sup>-1</sup>) in urban rivers following rainfalls<sup>25</sup>. However, other studies reported much lower concentrations of TiO<sub>2</sub> engineered particles in surface waters released from sunscreens (*e.g.*, 1.5-42.5 µg L<sup>-1</sup>)<sup>26-30</sup>. These discrepancies in the reported TiO<sub>2</sub> engineered particle concentrations can be ascribed to differences in sampling areas, the targeted source of TiO<sub>2</sub> engineered particles, and/or methodological differences<sup>2</sup>.

1  
2  
3 Monitoring engineered particle concentrations in the environment is challenging because of the  
4 similarities of physicochemical properties – such as composition, size, and shape – and the lower abundance  
5 of engineered particles compared to naturally occurring counterparts<sup>31,32</sup>. For instance, Ti is the ninth most  
6 abundant element in the Earth’s crust and is mainly found in minerals such as rutile, ilmenite, sphene, and/or  
7 opaque heavy minerals (*e.g.*, titanomagnetite, magnetite, and ilmenite)<sup>33</sup>. These minerals always contain  
8 trace concentrations of other elements such as Nb, Ta, Sn, Sb, W, V, Cr, Mo, and rare earth elements (REEs)  
9  
10  
11  
12  
13  
14  
15  
16  
17  
18  
19  
20  
21  
22  
23  
24  
25  
26  
27  
28  
29  
30  
31  
32  
33  
34  
35  
36  
37  
38  
39  
40  
41  
42  
43  
44  
45  
46  
47  
48  
49  
50  
51  
52  
53  
54  
55  
56  
57  
58  
59  
60

Monitoring engineered particle concentrations in the environment is challenging because of the similarities of physicochemical properties – such as composition, size, and shape – and the lower abundance of engineered particles compared to naturally occurring counterparts<sup>31,32</sup>. For instance, Ti is the ninth most abundant element in the Earth’s crust and is mainly found in minerals such as rutile, ilmenite, sphene, and/or opaque heavy minerals (*e.g.*, titanomagnetite, magnetite, and ilmenite)<sup>33</sup>. These minerals always contain trace concentrations of other elements such as Nb, Ta, Sn, Sb, W, V, Cr, Mo, and rare earth elements (REEs)<sup>34,35</sup>. These natural elemental impurities are typically removed from the natural Ti-bearing minerals during the manufacturing of TiO<sub>2</sub> engineered particles<sup>20</sup>. Thus, the introduction of TiO<sub>2</sub> engineered particles into environmental systems results in increases in the elemental ratios of Ti to those elements naturally occurring in Ti-bearing minerals (*e.g.*, Ti/Nb<sup>20,22,36,37</sup>, Ti/Al<sup>27</sup>, Ti/REEs<sup>27</sup>, and Ti/V<sup>23</sup>), which have been used to estimate the concentration TiO<sub>2</sub> engineered particles in environmental systems.

Multi element-single particle analysis by single particle-inductively coupled plasma-time of flight-mass spectrometer (SP-ICP-TOF-MS) is a promising technique in the nanometrology toolbox that has been implemented to differentiate ENPs from NNPs based on the subtle differences in their elemental composition<sup>20,38</sup>. The premise of ICP-TOF-MS is that it detects and quantifies all elements within a single particle at low/trace concentrations, and thus, SP-ICP-TOF-MS is the only method that could be implemented to differentiate ENPs from NNPs in environmental systems at the single particle level. However, the ability of the SP-ICP-TOF-MS to “unequivocally” differentiate ENPs from NNPs based on differences in elemental composition at the single particle level is challenged by the minimal detectable element mass (MDM), which is element dependent<sup>39,40</sup>. The MDM that can be attained by SP-ICP-MS depends on the instrument or elemental sensitivity and the background levels that result from both dissolved analyte and instrumental noise (electronic noise and interferences to the monitored isotope)<sup>40</sup>.

The overarching aim of this study is to evaluate the impact of urbanization on the concentrations of TiO<sub>2</sub> engineered particles in urban surface waters. To this end, we collected spatiotemporally resolved water samples from three Rivers within the urban zone of the city of Columbia, South Carolina, United States.

1  
2  
3 We then characterized these water samples for total elemental concentrations using ICP-TOF-MS,  
4 estimated the concentrations of anthropogenic TiO<sub>2</sub> engineered particles using mass balance calculations  
5 and shifts in elemental ratios above the natural background ratios, and determined particle elemental  
6 composition at the single particle level using SP-ICP-TOF-MS.  
7  
8  
9  
10

## 11 12 13 14 15 **2. Materials and Methods**

### 16 17 18 **2.1. Study area**

19  
20  
21 The confluence of the Lower Saluda and Broad Rivers forming the Congaree River at Columbia, South  
22 Carolina was selected as the study area to investigate the impact of urbanization on the concentrations of  
23 TiO<sub>2</sub> engineered particles in urban surface waters (**Figure 1**). Water samples were collected between  
24 27/4/2020 and 12/5/2020 from four locations within the limits of Columbia, South Carolina, United States,  
25 including the Lower Saluda River and the Broad River upstream of their confluence, and from Congaree  
26 River at Columbia and Cayce downstream of the Saluda and Broad Rivers' confluence. The Lower Saluda  
27 River (S) samples were collected near Hope ferry landing (34°02'45.7"N 81°11'27.3"W), approximately  
28 2.7 kms downstream of Lake Murray reservoir dam and 12.9 km upstream of the Lower Saluda and Broad  
29 Rivers' confluence. The Broad River (B) water samples were collected near Columbia rowing club  
30 (34°02'36.9"N 81°04'23.7"W), which is approximately 4.5 km upstream of the Saluda and Broad Rivers'  
31 confluence. The Congaree River Columbia samples were collected at West Columbia Riverwalk  
32 (33°59'35.4"N 81°03'1.8"W, Co), which is approximately 1.5 km downstream of the Saluda and Broad  
33 confluence. The Congaree River Cayce samples were collected at Thomas Newman public boat landing  
34 (33°56'57.3"N 81°01'44.1"W, C), which is approximately 6.8 km downstream of the Saluda and Broad  
35 Rivers' confluence. This sampling area captures a significant footprint of the urban area - accounting for  
36 approximately 50% - of the city of Columbia, South Carolina, United States. A detailed description of the  
37  
38  
39  
40  
41  
42  
43  
44  
45  
46  
47  
48  
49  
50  
51  
52  
53  
54  
55  
56  
57  
58  
59  
60

1  
2  
3 sampling locations including land use, industrial-commercial activities, mining activities, wastewater and  
4 storm water facilities in the watershed is provided in the supplementary information section S11.  
5  
6

7  
8 Precipitation data for the Broad and Congaree Rivers' sampling locations was collected from the USGS  
9 station number 021695045 (34°00'24"N 81°01'18"W), nearly 6.3 km from the Broad River sampling  
10 location, and nearly 3.1 km from the Congaree River Columbia sampling location and 6.4 km from the  
11 Congaree River Cayce sampling location. Rainfall and discharge data for the Lower Saluda River sampling  
12 location were collected from USGS station number 02168504 (34°03'03"N 81°12'35"W) immediately after  
13 the dam and nearly 1.8 km upstream from the Lower Saluda River sampling location. The discharge data  
14 for the Broad and Congaree Rivers was collected from the USGS stations' number 02162035 (34°02'54"N  
15 81°04'24"W) and 02169500 (33°59'35"N 81°03'00"W), nearly 5.3 km upstream of the Broad River  
16 sampling location and 0.05 km upstream from the Congaree River Columbia sampling location and 5.3 km  
17 upstream from the Congaree River Cayce sampling location, respectively.  
18  
19  
20  
21  
22  
23  
24  
25  
26  
27  
28

## 29 **2.2. Sample collection, digestion, and elemental analysis**

30  
31

32  
33 Surface water samples were collected from the Broad, Lower Saluda, and Congaree Rivers in 250-mL  
34 high density polyethylene bottles (Thermo Scientific, Rockwood, TN, United States). Prior to use, bottles  
35 were acid-washed in 10% nitric acid (Sigma Aldrich, St. Louis, MO, United States) for at least 24 hours,  
36 and soaked in ultrahigh purity water (PURELAB Option-Q, ELGA, High Wycombe, UK) for 24 hours, air  
37 dried, and double-bagged. In the field, sampling bottles were rinsed three times in the surface water and  
38 then filled with the water sample. Samples were individually double-bagged and returned to the lab the  
39 same day and stored in the dark at 4°C.  
40  
41  
42  
43  
44  
45  
46  
47

48 The bulk water samples were digested using a mixture of H<sub>2</sub>O<sub>2</sub>, HNO<sub>3</sub>, and HF following the digestion  
49 protocol described elsewhere and summarized in the SI section 2<sup>17,22,37</sup>. Elemental concentrations in the  
50 digested samples were determined by ICP-TOFR ICP-TOF-MS (TOFWERK, Switzerland) using TOFPilot  
51 2.8.8 software. The instrument operating conditions are presented in **Table S3**. Mass spectra calibration  
52  
53  
54  
55  
56  
57



1  
2  
3 and standard tuning procedure were performed before analysis for instrument maintenance. Dissolved  
4 multi-element standards were prepared in 1% HNO<sub>3</sub> from commercially available ICP standards (BDH  
5 Chemicals, Radnor, PA, USA) with concentrations ranging from 0.001 to 100 µg L<sup>-1</sup>. Internal standards  
6 (ICP Internal Element Group Calibration Standard, BDH Chemicals, Radnor, PA, USA) were monitored at  
7 the same time for quality control. The isotopes measured were <sup>27</sup>Al, <sup>49</sup>Ti, <sup>57</sup>Fe, <sup>90</sup>Zr, <sup>93</sup>Nb, <sup>139</sup>La, <sup>140</sup>Ce, <sup>141</sup>Pr,  
8 <sup>142</sup>Nd, <sup>152</sup>Sm, <sup>153</sup>Eu, <sup>158</sup>Gd, <sup>159</sup>Tb, <sup>164</sup>Dy, <sup>165</sup>Ho, <sup>166</sup>Er, <sup>169</sup>Tm, <sup>174</sup>Yb, and <sup>175</sup>Lu. The minor isotopes (*e.g.*, <sup>49</sup>Ti  
9 and <sup>57</sup>Fe) instead of the major isotopes (*e.g.*, <sup>48</sup>Ti and <sup>56</sup>Fe) were used to determine the concentrations of Ti  
10 and Fe to avoid potential isobaric element and polyatomic ion interferences with <sup>48</sup>Ca<sup>+</sup> and <sup>40</sup>Ar<sup>16</sup>O<sup>+</sup>,  
11 respectively. All isotopes were analyzed in collision/reaction mode.  
12  
13  
14  
15  
16  
17  
18  
19  
20  
21  
22

23 The USGS reference material BHVO-2 Hawaiian basalt was digested following the same procedure  
24 described above. The elemental analysis of the reference material demonstrated high recovery  
25 (approximately 100%) for most elements. The precision of our method was within 8% for all isotopes and  
26 the accuracy was better than 89% for most elements, including Ti and Nb. Full procedural digestion blanks  
27 was < 6.8% samples' analyte signal for all reported element in this study and < 2.8% samples' analyte  
28 signal for Ti and Nb (**Table S4**). Therefore, blanks are insignificant to the calculations of Ti concentrations  
29 or total Ti/Nb elemental ratios.  
30  
31  
32  
33  
34  
35  
36  
37

### 38 **2.3. Particle composition on single particle basis**

39  
40

41 The multi-elemental composition of individual particles in a select set of samples (*e.g.*, 30/4/2020,  
42 1/5/2020, 2/5/2020, and 5/5/2020) representing the start, rising limb, peak, and end of the first runoff event  
43 in the studied river system was determined using SP-ICP-TOF-MS. The river water samples were shaken  
44 well prior to extraction to resuspend any settled particles and to obtain a representative subsample. The  
45 extraction procedure is the same as that used in previous studies<sup>17,22,37</sup>. Briefly, 10 mL aliquots of the river  
46 water samples were transferred into acid-washed 15 mL centrifuge tubes. Then, the samples were bath  
47 sonicated for 2 h (Branson, Model 2800, 40 kHz, Danbury, CT, United States) and centrifuged at 775 g for  
48  
49  
50  
51  
52  
53  
54  
55  
56  
57  
58  
59  
60

1  
2  
3 5 min (Eppendorf Centrifuge 5810R, Hamburg, Germany) to obtain the  $< 1 \mu\text{m}$  particle size fraction  
4  
5 (assuming natural particle density of  $2.5 \text{ g cm}^{-3}$ ). The theoretical equivalent spherical diameter of the  
6  
7 extracted fractions corresponds to particles  $< 1000 \text{ nm}$  for natural particles ( $\rho = 2.5 \text{ g cm}^{-3}$ ), and  $< 725 \text{ nm}$   
8  
9 for  $\text{TiO}_2$  particles ( $\rho = 4.2 \text{ g cm}^{-3}$ ). All samples were bath sonicated again for 15 min and were diluted by a  
10  
11 factor of 100 prior to SP-ICP-TOF-MS analysis.  
12  
13

14  
15 Similar to the total elemental analysis, the instrument was calibrated and tuned daily before single  
16  
17 particle analysis. Transport efficiency was calculated based on analysis of certified Au ENPs (NIST  
18  
19 RM8013 Au, Gaithersburg, MD, USA) and ionic Au standards <sup>41</sup>. Dissolved element calibration was  
20  
21 performed using a series of mixed multi-element standards (0, 1, 2, 5, and  $10 \mu\text{g L}^{-1}$ , BDH Chemicals,  
22  
23 Radnor, PA, USA). Particle signals were separated from baseline using TOFpilot V2.10 and reported in  
24  
25 time-elapsed format.  
26  
27

28  
29 The detected particles were classified into single- and multi-metals (smNPs and mmNPs). The smNPs  
30  
31 were considered as their own clusters because the particle mass and number concentrations are not sufficient  
32  
33 to cluster smNPs. The mmNPs were classified into clusters of NPs of similar elemental composition using  
34  
35 a two stage - intra- and inter- sample - agglomerative hierarchical clustering algorithm in MATLAB  
36  
37 following the method described elsewhere <sup>42</sup>. Briefly, intra-sample hierarchical clustering was performed -  
38  
39 using average correlation distance - on all metal masses in each NP to generate clusters that best account  
40  
41 for variance in NP metallic composition in each sample. This step generates a cluster dendrogram for each  
42  
43 sample, which was divided into major clusters using a distance cutoff. The distance cutoff of 0.65, was  
44  
45 determined by visually inspecting the dendrogram and through trial and error in order to minimize the  
46  
47 variance/diversity in NP elemental composition in the major clusters. A cluster representative was  
48  
49 determined for each major cluster as the mean of metal mass in individual NPs within each cluster taking  
50  
51 into account all elements that occurred in at least 5 percent of NPs within the cluster. For each major cluster,  
52  
53 the mass fraction of a given metal in each particle was determined as the mass of that metal divided by the  
54  
55 sum of masses of all metals in that NP. The inter-sample clustering was performed on the major cluster  
56  
57

representatives identified in the intra-sample clustering to group/cluster the similar NP major clusters identified in the different samples. This step generates a cluster dendrogram for intra-sample cluster representatives, which was divided into major clusters using a distance cutoff as performed for the intra sample clusters. The distance cutoff of 0.2, was determined by visually inspecting the dendrogram and through trial and error in order to minimize the variance/diversity in the cluster representative elemental composition in the major clusters. The mean intra-sample cluster composition was determined as the mean of metal mass fraction in all NPs in the cluster and was compared across samples. Select elemental ratios were determined on a particle-per-particle basis taking into account all particles containing the two elements. The number concentration (NP g<sup>-1</sup>) of the total, smNPs, mmNPs, and cluster members were determined according to the SP-ICP-MS theory <sup>41</sup>.

## 2.4. Estimation of TiO<sub>2</sub> engineered particle concentration

The concentration of TiO<sub>2</sub> engineered particles was calculated based on mass balance calculations according to Eq. 1

$$[TiO_2]_{engineered\ particles} = \frac{TiO_2_{MM}}{Ti_{MM}} \left[ Ti_{sample} - Nb_{sample} \cdot \left( \frac{Ti}{Nb} \right)_{background} \right] \quad (Eq. 1)$$

Where,  $[TiO_2]_{engineered\ particles}$  is the concentration of TiO<sub>2</sub> engineered particles (μg L<sup>-1</sup>),  $Ti_{MM}$  and  $TiO_2_{MM}$  are the molar masses of Ti and TiO<sub>2</sub>,  $Ti_{sample}$  and  $Nb_{sample}$  are the concentrations (μg L<sup>-1</sup>) of Ti and Nb in a given sample,  $(Ti/Nb)_{background}$  is the natural background elemental concentration ratio of Ti/Nb. Background Ti/Nb was calculated on eight reference samples collected from Lake Katherine and Gills creek in Columbia, SC in the absence of rainfall events <sup>20</sup>. Eq 1 assumes that all Ti occurs in particulate form, engineered Ti occurs as pure TiO<sub>2</sub> engineered particles, and that the natural background Ti/Nb is constant throughout the sampling period. These assumptions are justified for the following reasons. Ti occurrence in the surface waters is expected to occur solely in solid phases because of the very low solubility of TiO<sub>2</sub> <sup>43</sup>. While Ti has numerous industrial applications, from metal alloying to aerospace applications to biomedical devices, approximately 95% of the mined Ti is refined into nearly pure TiO<sub>2</sub> through the

1  
2  
3 treatment of Ti-bearing ores with carbon, chlorine, or sulfuric acid<sup>44</sup>. Additionally, TiO<sub>2</sub> engineered particle  
4 contain trace amount of Nb, which was below the ICP-MS detection limit (*e.g.*, < 7 ng L<sup>-1</sup>) for TiO<sub>2</sub>  
5 concentration upto 10,000 mg L<sup>-1</sup><sup>22</sup>. On the other hand, natural TiO<sub>2</sub> minerals are the dominant carriers  
6 (*e.g.*, > 90-95% of the whole rock content) of Ti and Nb. The elemental ratios of Ti/Fe, Ti/Al, Ti/Ce, Ti/Zr,  
7 and Ti/Nb, determined by SP-ICP-TOF-MS, in naturally occurring particles in the Broad, Lower Saluda,  
8 and Congaree Rivers were found to be within the range of naturally occurring particles throughout the  
9 sampling campaigns (see discussion below and supplementary information).  
10  
11  
12  
13  
14  
15  
16  
17

## 18 **2.5. Discharge hydrographs and baseflow estimation**

19  
20  
21 The discharge was separated into baseflow and direct runoff using the tool “WHAT: Web-based  
22 Hydrograph Analysis Tool”. ‘WHAT’ is able to connect to the USGS database and query and analyze  
23 streamflow data based on its USGS gauge number. The baseflow and direct runoff separation for the Broad,  
24 Lower Saluda, and Congaree Rivers was performed for the USGS station number 02162035, 02168504,  
25 and 02169500, respectively. For baseflow separation, recursive digital filter has been used with aquifer type  
26 of perennial streams with porous aquifer.  
27  
28  
29  
30  
31  
32  
33  
34

## 35 **3. Results**

### 36 **3.1. Precipitation, discharge, runoff, and water quality**

37  
38  
39  
40  
41 A significant rain event occurred on 30/4/2020 resulting in 16.8 mm, 15.7 mm, and 16.8 mm rainfall in  
42 the Broad, Lower Saluda, and Congaree River watersheds respectively. Smaller rain events of 0.5, 0.5, and  
43 1.0 mm occurred on 29/4/2020, 5/5/2020, and 10/5/2020 in the Broad, Lower Saluda, and Congaree River  
44 watersheds, respectively (**Table S5**). Moreover, major rainfall events of 40.2 mm and 9.7 mm occurred on  
45 29/4/2020 in the upstream region of the Broad River at Ashville, NC and Knoxville, TN respectively<sup>45,46</sup>;  
46 and 54.5 mm and 3.1 mm occurred on 29/4/2020 and 30/4/2020 in the upstream region of the Lower Saluda  
47 River at Rock reservoir, Cleveland, SC<sup>47</sup>. These rain events resulted in increases in release from upstream  
48 reservoirs and as a result increases in the discharge in the Lower Saluda, Broad, and Congaree Rivers (**Table**  
49  
50  
51  
52  
53  
54  
55  
56  
57  
58  
59  
60

1  
2  
3 **S5; Figure S1**). During this period, water level behind the Lake Murray dam was about 109 m above datum,  
4 which is very close to the top of conservation (flood control level of ~109.1 m) of the dam. The discharge  
5 in the Lower Saluda River is dominated by regulated releases from the Lake Murray reservoir based on the  
6 required hydroelectric power generation and flood control regulations. Thus, the discharge in the Lower  
7 Saluda River displayed sharp increases between 30/4/2020 and 1/5/2020 and between 4/5/202 and 9/5/2020  
8 due to releases from the Lake Murray reservoir in anticipation of the rain events to keep water level behind  
9 the dam below flood zone level (**Table S5; Figure S1**). Lake Murray is a man-made reservoir of  
10 approximately 200 km<sup>2</sup> in size with a maximum depth of approximately 53 m, an average depth of  
11 approximately 14 m, and a residence time of approximately 417 days<sup>48,49</sup>. The majority of the inflow to  
12 Lake Murray comes from releases from upstream dams on Saluda River as well as rainfall over the lake.  
13 Local tributaries, which are mostly rural basins, contribute minimally to the storage behind the Lake Murray  
14 dam. Thus, the urban contribution at the sampling point to the total discharge is minimal.

15  
16  
17  
18  
19  
20  
21  
22  
23  
24  
25  
26  
27  
28  
29 The discharge in the Broad and the Congaree Rivers display typical hydrographs of natural river  
30 discharges. The Broad River is regulated to some degree by the presence of at least 10 hydroelectric  
31 facilities and two thermoelectric power plants (**Table S1**)<sup>50</sup>. The upstream of Broad River from sampling  
32 point is regulated using the Parr reservoir dam, approximately 40 km upstream of the sampling location,  
33 which operates in modified run-of-river mode and operates continuously to pass the Broad River flow.  
34 These facilities allow a natural river flow to downstream<sup>51</sup>. The retention time of Parr Reservoir is on  
35 average about 3 days and varies between 0.8 and 29.3 days based on a maximum and minimum monthly  
36 flow of 530 and 15 m<sup>3</sup> sec<sup>-1</sup>, respectively<sup>52</sup>. The nearest dam to the sampling location is the Broad River  
37 diversion dam (low head, a constructed barrier in a river with a hydraulic height not exceeding 7.6 m),  
38 approximately 4 km upstream of the Broad River sampling site. This dam diverts the flow (long term  
39 average diversion of approximately 11.7 m<sup>3</sup> sec<sup>-1</sup>) of the Broad River toward the canal of the Columbia  
40 Hydroelectric Project. The rainfall resulted in runoff discharges in the Broad and Congaree Rivers between  
41 30/4/2020 and 4/5/2020 and between 5/5/2020 and 9/5/2020 with peak discharge on 1/5/2020 and 7/5/2020.  
42  
43  
44  
45  
46  
47  
48  
49  
50  
51  
52  
53  
54  
55  
56  
57  
58  
59  
60

1  
2  
3 Direct runoff accounted for < 6%, 9-77%, 8-75% of the total discharge in the Lower Saluda, Broad, and  
4 Congaree River, respectively. The highest runoff contribution (*e.g.*, direct runoff/total discharge) in the  
5 Broad and Congaree Rivers occurred on 1/5/2020. There has been no urban runoff contribution (*i.e.*,  
6 baseline flow occurred) on 27/4/2020, 10/5/2020, and 12/5/2020 in the Broad and Congaree Rivers. The  
7 average annual discharge rates at the Broad River and Congaree River Columbia sampling sites are  
8 approximately 163.08 m<sup>3</sup> sec<sup>-1</sup> and 243.86 m<sup>3</sup> sec<sup>-1</sup>. We estimated the urban contribution from the city of  
9 Columbia between the Broad and Congaree Rivers' sampling sites as the difference between the sum of the  
10 discharge at the Congaree River sampling location and the water withdrawal at the Broad River diversion  
11 dam (approximately 255.56 m<sup>3</sup> sec<sup>-1</sup>) and the sum of the discharge at the Broad River and Lower Saluda  
12 River sampling locations (approximately 225.68 m<sup>3</sup> sec<sup>-1</sup>). The average annual runoff contribution of the  
13 city of Columbia is approximately 29.88 m<sup>3</sup> sec<sup>-1</sup>.  
14  
15  
16  
17  
18  
19  
20  
21  
22  
23  
24  
25

26  
27 The pH varied in a narrow range between 6.4 and 7.8 and is similar in all samples (**Figure S2a**). The  
28 conductivity vary between 48 and 119  $\mu\text{s cm}^{-1}$  with higher values on 27/4/2020 and 28/4/2020 and relatively  
29 stable values of around 55  $\mu\text{s cm}^{-1}$  between 29/4/2020 and 12/5/2020 (**Figure S2b**). The water temperature  
30 in the Lower Saluda River water was lower than those in the Broad and Congaree Rivers as the water comes  
31 from deep in Lake Murray reservoir (**Figure S2c**).  
32  
33  
34  
35  
36  
37  
38

### 39 3.2. Total Ti, Nb, and TiO<sub>2</sub> concentrations

40  
41 Titanium and Niobium concentrations in the Lower Saluda, Broad, and Congaree Rivers during the  
42 sampling period are presented in **Figure 2a and b**. Titanium concentrations vary randomly within a narrow  
43 range in the Lower Saluda River between 13 and 60  $\mu\text{g L}^{-1}$  (**Figure 2a**) and does not follow a specific trend  
44 in relation to the discharge. In contrast, titanium concentrations vary within a broader range in the Broad  
45 and Congaree Rivers at Columbia and Cayce (8 to 926  $\mu\text{g L}^{-1}$ , 95 to 5976  $\mu\text{g L}^{-1}$ , and 58 to 1170  $\mu\text{g L}^{-1}$ ,  
46 respectively). The concentrations of Ti in the Broad River follow the discharge trend and continue rising  
47 after the second discharge peak. The reason for the increase in Ti concentration after the second discharge  
48  
49  
50  
51  
52  
53  
54  
55  
56  
57  
58  
59  
60

1  
2  
3 peak is unknown. The concentrations of Ti in the Congaree River at Columbia and Cayce display a bimodal  
4 distribution and follow closely the rise and fall of the discharge. The highest Ti concentration in the  
5 Congaree River at Columbia and Cayce was measured on 1/5/2020 and 2/5/2020, respectively. Generally,  
6 Ti concentrations decrease following the order: Congaree River at Columbia > Congaree River at Cayce >  
7 Broad River > Lower Saluda River, which is scribed to differences in Ti load into these rivers due to  
8 differences in urban runoff contribution to the total discharge. The Nb concentrations follow the same trend  
9 as that of Ti (**Figure 2b**). Ti and Nb pollutographs in the Broad and Congaree Rivers display a mobility  
10 pattern driven by the transport of solids<sup>53</sup>; that is the Ti and Nb concentrations are low during low flows,  
11 increase with increasing flow due to the transportation of more solids, and then decline with diminishing  
12 flow and supply of solids on the catchment surfaces (**Figure 2**).

13  
14  
15  
16  
17  
18  
19  
20  
21  
22  
23  
24  
25 In the Lower Saluda River, the Ti/Nb ratios vary between  $238.8 \pm 12.1$  and  $346.7 \pm 2.4$  and do not follow  
26 specific trend with the discharge (**Figure 2c**). In the Broad and Congaree Rivers, the Ti/Nb ratios display a  
27 bimodal distribution and increase with increases and decreases in the discharge/runoff. The general increase  
28 in Ti/Nb ratios over time can be attributed to the continuous runoff input during the sampling period. The  
29 Ti/Nb values increase following the order Lower Saluda River < Broad River < Congaree River at Columbia  
30 < Congaree River at Cayce. This trend in Ti/Nb ratios is attributed to the introduction of anthropogenic  
31 pure Ti-bearing particles between the sampling sites, which can be ascribed to urban runoff from the City  
32 of Columbia. The concentration of the anthropogenic Ti-bearing particles was estimated using mass balance  
33 and assuming that they occurred as pure  $\text{TiO}_2$  particles. The estimated anthropogenic  $\text{TiO}_2$  concentrations  
34 vary between 0 and  $24 \mu\text{g L}^{-1}$  in the Lower Saluda River, 0 and  $663 \mu\text{g L}^{-1}$  in the Broad River, 58 and  $5050$   
35  $\mu\text{g L}^{-1}$  in the Congaree River at Columbia, and 43 to  $1051 \mu\text{g L}^{-1}$  in the Congaree River at Cayce; and follow  
36 the same trend with discharge/direct runoff as the total Ti concentrations (**Figure 2d**).

### 3.3. Particle number concentrations and elemental composition

37  
38  
39  
40  
41  
42  
43  
44  
45  
46  
47  
48  
49  
50  
51  
52  
53  
54  
55  
56  
57  
58  
59  
60

1  
2  
3 The number concentrations of Ti-bearing particles are generally higher in the Broad and Congaree  
4 Rivers compared to those in the Lower Saluda River (**Figure 3a**). The relative abundance of smTi-NPs is  
5 generally higher during the first discharge event than at the end of the event (**Figure 3b**). All other elements  
6 follow the same trend as Ti-bearing particles (**Figure S3**). Due to the complex nature of the SP-ICP-TOF-  
7 MS, only a select set of four samples per sampling site during the first discharge peak were analyzed to  
8 determine the elemental composition of NP at the single particle level. Therefore, it is not possible to  
9 compare the relative abundance of smNPs before the discharge to that during the discharge peak. The  
10 mass distributions of Ti-bearing particles vary within the same range (*e.g.*, 0 to 20 fg) in all samples (**Figure**  
11 **4**). However, the mass distributions of Ti-bearing particles in the Broad and Congaree Rivers display a  
12 shift toward larger masses compared to those in the Lower Saluda River, with a higher fraction of particles  
13 with mass > 20 fg. The mass distributions of Ti-bearing particles in the Congaree River at Columbia is  
14 intermediate between those in the Broad and the Lower Saluda Rivers due to the mixing of the two Rivers  
15 upstream of this sampling location (**Figure 4**). The mass distributions of Ti-bearing particles shift toward  
16 higher masses during high discharge (1/5/2020 and 2/5/2020) compared to those at low discharge  
17 (30/4/2020 and 5/5/2020). The mass distributions of smTi and mmTi-bearing particles cover the same mass  
18 distribution range with a higher abundance of Ti particles with larger masses for mmTi-bearing than smTi-  
19 bearing particles (**Figure S4**). This can be attributed to the higher probability of detecting naturally  
20 occurring elements in natural mmTi-bearing particles or to the heteroaggregation of smTi- and mmTi- or  
21 the heteroaggregation of multiple mmTi-bearing particles.

22  
23  
24  
25  
26  
27  
28  
29  
30  
31  
32  
33  
34  
35  
36  
37  
38  
39  
40  
41  
42  
43 Clustering analysis of the mmNPs identified 29 mmNP clusters. Six of these 29 clusters - FeTiMn,  
44 AlSiFe, CeLaNd, TiMnFe, MnCeBa, and ZrYTh – occur in all samples and account for > 99.4% of the  
45 total number of mmNPs in all samples (**Figure S5**). The elemental composition of these clusters is  
46 dominated by one element and contain minor or trace concentrations of other elements (**Figure 5**)<sup>54</sup>. The  
47 Ti-bearing particles are distributed among three clusters: FeTiMn, AlSiFe, and TiMnFe, which account for  
48 > 99% of all mm-Ti-bearing NPs (**Figure S5**). The elemental ratios of Ti/Fe, Ti/Al, Ti/Ce, Ti/Zr, and Ti/Nb  
49  
50  
51  
52  
53  
54  
55  
56  
57  
58  
59  
60



1  
2  
3 are similar in all samples and are in good agreement with those measured in natural soils and surface waters  
4  
5 **(Figure S6-8)**<sup>20,54,55</sup>. The median values of Ti/Fe, Ti/Al, Ti/Ce, Ti/Zr, and Ti/Nb varies within the range of  
6  
7 those measured in of natural soils and surface waters **(Table S6-8)**<sup>20,54,55</sup>. The mean Ti/Nb ratio in all Ti  
8  
9 and Nb containing particles in all samples vary between (mean  $\pm$  standard deviation of the ratios calculated  
10  
11 at the single particle level)  $218 \pm 195$  and  $295 \pm 280$ .  
12  
13  
14  
15  
16

#### 17 **4. Discussion**

18  
19  
20 The lowest Ti concentration in the Lower Saluda, Broad, and Congaree (Co) Rivers are  $13.3 \pm 0.2 \mu\text{g}$   
21  
22  $\text{L}^{-1}$ ,  $8.2 \pm 0.1 \mu\text{g L}^{-1}$ , and  $94.8 \pm 27.1 \mu\text{g L}^{-1}$  respectively and occurred during base flow dominated condition  
23  
24 when base flow accounted for 90.5%, 100%, and 68% of the total discharge, respectively **(Figure 2a)**. The  
25  
26 highest Ti concentration in the Lower Saluda, Broad, and Congaree (Co) Rivers are  $39.2 \pm 6.7 \mu\text{g L}^{-1}$ ,  $233.4$   
27  
28  $\pm 8.1 \mu\text{g L}^{-1}$  and  $5975.7 \pm 88.8 \mu\text{g L}^{-1}$  respectively and coincided with the peak discharge during the first  
29  
30 runoff event on 1/5/2020 **(Figure 2a)**. The low concentration of Ti in the Saluda River, which is  
31  
32 characterized by minimal urban runoff contribution to the total discharge, and the increase in Ti  
33  
34 concentration from the Broad River to the Congaree River, which are characterized by high urban runoff  
35  
36 contribution to the total discharge, suggest that urban runoff is the key driver of Ti concentrations in the  
37  
38 Broad and Congaree Rivers. The Ti concentrations measured in this study are higher than those previously  
39  
40 measured in rivers (*e.g.*  $0.6$  to  $1.6 \mu\text{g L}^{-1}$ )<sup>56</sup>, urban runoff (*e.g.*,  $10$  to  $15 \mu\text{g L}^{-1}$ ) following the release of  
41  
42  $\text{TiO}_2$  particles from exterior facades<sup>57</sup>, and urban wet and dry runoff (*e.g.*,  $15$  to  $200 \mu\text{g L}^{-1}$ )<sup>17</sup>. Nonetheless,  
43  
44 higher Ti concentrations (*e.g.*,  $12.7 \text{ mg L}^{-1}$ ) were reported in highway runoff in Pullman, Washington<sup>19</sup>.  
45  
46 Additionally, high Ti concentrations (*e.g.*,  $150$  to  $1600 \text{ mg kg}^{-1}$ ) were reported in different road-environment  
47  
48 samples (*e.g.*, road dust, sludge from storm drains, and roadside soil), which were suspected to be of  
49  
50 anthropogenic origin such as the use of alkali metal titanates as inorganic fillers for the purpose of  
51  
52 stabilizing the friction coefficient<sup>58</sup>.  
53  
54  
55  
56  
57  
58  
59  
60

1  
2  
3 Titanium in urban runoff can be attributed to natural and/or anthropogenic sources. Significant quantities  
4 of Ti-bearing particles occur in the urban environment due to the soil erosion and atmospheric deposition  
5 of soil particles on surfaces in the urban environment<sup>59</sup>. On the other hand, TiO<sub>2</sub> engineered particles are  
6 widely used in many applications in the urban environment as pigment in paint and coatings<sup>60,61</sup> and as  
7 ENPs in self-cleaning surfaces which have been shown to be released by wear and weathering<sup>5-9</sup>. Several  
8 studies reported the occurrence of TiO<sub>2</sub> engineered (nano)-particles in road dust, atmospheric particulate  
9 matter<sup>62,63</sup>, and urban runoff<sup>17</sup>. Whereas naturally occurring TiO<sub>2</sub> minerals are the dominant carriers of Ti  
10 and Nb<sup>34</sup>, commercial TiO<sub>2</sub> particles are typically refined into nearly pure TiO<sub>2</sub><sup>22,64</sup>. Thus, the elemental  
11 ratio of Ti/Nb was used to determine whether the increased Ti concentration is due to natural or  
12 anthropogenic Ti inputs. The Ti/Nb in most samples is higher than the natural background ratio determined  
13 in a previous study (**Figure 2c**)<sup>20</sup>, suggesting that all sampling locations received anthropogenic Ti inputs.  
14 The lowest Ti/Nb ratios occurred in the Lower Saluda River ( $239 \pm 12$ ) and coincided with the average  
15 water background Ti/Nb determined in nearby water bodies ( $266 \pm 9$ )<sup>20</sup>. The higher (*e.g.*, 280-346) Ti/Nb  
16 values in the Lower Saluda River indicate a potential small anthropogenic contribution of TiO<sub>2</sub> engineered  
17 particles, potentially from atmospheric deposition or urban runoff from nearby roads and bridges. The  
18 lowest Ti/Nb in the Broad and Congaree Rivers ( $177 \pm 36$ ,  $408 \pm 17$ , and  $435 \pm 19$ , respectively) occurred  
19 at the base flow conditions. On the other hand, the highest Ti/Nb ratios ( $503 \pm 5$ ,  $596 \pm 11$ , and  $688 \pm 31$ )  
20 occurred at the peak of the discharge events on 1/5/2020 and 7/5 2020, suggesting that the discharge/urban  
21 runoff is the driver of the increase in Ti/Nb during/following rainfall events. The lower Ti/Nb ratios in the  
22 Lower Saluda River than in the Broad and Congaree Rivers are ascribed to the smaller urban runoff  
23 contribution to the Lower Saluda River discharge at the sampling location along with sedimentation of  
24 anthropogenic Ti-bearing particles in Lake Murray, and thus low input of anthropogenic Ti to the Lower  
25 Saluda River.  
26  
27  
28  
29  
30  
31  
32  
33  
34  
35  
36  
37  
38  
39  
40  
41  
42  
43  
44  
45  
46  
47  
48  
49  
50

51  
52 The anthropogenic Ti-bearing particles from urban runoff can occur as smNPs such as those used in  
53 building paint, road marking, and photocatalytic surfaces or as mmNPs as those released from traffic-related  
54  
55  
56  
57  
58  
59  
60

1  
2  
3 emissions such as Ti used as fillers in brake pads. Thus, SP-ICP-TOF-MS analysis was used to determine  
4 the elemental composition of Ti-bearing particles. The SP-ICP-TOF-MS analysis show higher relative  
5 abundance of smTi-bearing NPs during the runoff event than at the end of the runoff event (**Figure 3b**) in  
6 all sampling sites, which can be ascribed to the increased contribution of pure TiO<sub>2</sub> particles to the total  
7 concentration of Ti-bearing particles during the runoff event. The clustering and elemental ratio analysis  
8 show that > 99% of mm-Ti-bearing particles occurred in three clusters (FeTiMn, AlSiFe, TiMnFe), which  
9 are typical of naturally occurring particles such as titanomagnetite (Ti/Fe = 0 to 0.43), ilmenite (Ti/Fe =  
10 0.86), pseudorutile (Ti/Fe = 1.29), Ilmenorutile (Ti/Fe = 1.71), or altered pseudorutile (Ti/Fe > 1.71)  
11 (**Figure S6a and S7a**), clays (Ti/Al = 0 to 0.4, **Figure S6a and S7a**), or titanium oxide particles containing  
12 Al and Fe (**Figure S8**). The higher bulk Ti/Nb than the natural background ratio and the absence of any  
13 signature of anthropogenic mmTi-bearing NPs suggest that the majority of anthropogenic Ti-bearing  
14 particles are pure TiO<sub>2</sub> particles. It is worth noting that other clusters such as Zn, Cu, Cr, W, Ni, Sn-rich  
15 particle clusters were identified more frequently in the Broad and Congaree Rivers than in the Lower Saluda  
16 River (**Figure S5**). These particles are typical of traffic related emissions detected in bridge runoff in  
17 Columbia, South Carolina <sup>36</sup>. However, the number of the detected particles are relatively small and thus  
18 these clusters are not discussed further.

19  
20  
21  
22  
23  
24  
25  
26  
27  
28  
29  
30  
31  
32  
33  
34  
35  
36  
37  
38  
39  
40  
41  
42  
43  
44  
45  
46  
47  
48  
49  
50  
51  
52  
53  
54  
55  
56  
57  
58  
59  
60

Consequently, the total TiO<sub>2</sub> engineered particle concentrations were determined using mass balance calculations and shifts in Ti/Nb above the natural background values (**Figure 2d**). The lower concentrations of TiO<sub>2</sub> engineered particles in the Lower Saluda River compared to the Broad and Congaree Rivers can be attributed to the removal of suspended sediments and anthropogenic TiO<sub>2</sub> particles within the Lake Murray reservoir by sedimentation given the long water residence time of approximately 417 days <sup>48,49</sup>. This is consistent with the decreases in turbidity from upstream to downstream Lake Murray reservoir <sup>48,49</sup>. This is also consistent with the smaller masses of Ti-bearing particles in the Lower Saluda River compared to those in the Broad and Congaree Rivers (**Figure 4**). Additionally, the low TiO<sub>2</sub> concentration in the Lower Saluda River can be attributed to the absence or small urban runoff contribution (~ 6%) to the discharge at the

1  
2  
3 Lower Saluda River sampling location. In contrast, the Broad River is a natural free flowing river which  
4 transports a higher sediment load into the Broad River sampling location from the large upstream Broad  
5 River watershed. Additionally, the Broad River sampling site is approximately 480 m downstream of a  
6 major highway in South Carolina – that is the interstate I20 bridge – which discharges directly into the  
7 Broad River. Our previous study demonstrated that bridge runoff contains high concentrations of  
8 anthropogenic TiO<sub>2</sub> particles <sup>65</sup>.  
9  
10  
11  
12  
13  
14  
15

16 The increase in TiO<sub>2</sub> concentration from the Broad River to the Congaree River for most sampling dates  
17 suggests that the majority of anthropogenic TiO<sub>2</sub> is introduced into the Broad and Congaree Rivers at the  
18 urban interface area of the city Columbia, SC, and is ascribed to urban runoff and associated particulate  
19 wash off from impervious surfaces. This is consistent with the significant contribution of urban runoff to  
20 the total discharge in the Broad River (*e.g.*, 9-77%) and the Congaree Rivers (*e.g.*, 8-75%) as well as the  
21 high concentrations of TiO<sub>2</sub> in bridge and urban runoff <sup>17</sup>. The Broad River sample was collected  
22 downstream of the I20 highway; the Congaree River at Columbia sample was collected downstream of  
23 I176, I126, the Jarvis Klapman Boulevard, and the Gervais Bridges; and the Congaree River at Cayce  
24 sample was collected downstream of Blossom Street Bridge. All these bridges have an AADT > 20,000,  
25 which result in a substantial release of TiO<sub>2</sub> to the studied river system (**Table S2**). For instance, the  
26 Blossom Street Bridge (AADT = 27,500) runoff has been shown to contain up to 101.1 ± 1.4 µg TiO<sub>2</sub> L<sup>-1</sup>  
27 <sup>36</sup>. It is expected that Bridges with higher traffic density will release higher concentrations of TiO<sub>2</sub> to the  
28 studied river system. The lower TiO<sub>2</sub> concentration in the Congaree River than in the Broad River between  
29 10/5/2020 and 12/5/2020 could be due to dilution effect because of the mixing of the Broad River water  
30 containing high TiO<sub>2</sub> concentrations with the Saluda River water containing low TiO<sub>2</sub> concentrations.  
31  
32  
33  
34  
35  
36  
37  
38  
39  
40  
41  
42  
43  
44  
45  
46  
47

48 The higher TiO<sub>2</sub> concentrations during the first discharge peak than during the second discharge peak  
49 in the Congaree River is attributed to the relatively longer antecedent dry period (**Table S5**) prior to the  
50 first rainfall event. Longer antecedent dry periods lead to higher contaminant accumulation on impervious  
51 surfaces in the watershed. The heavy rain event on the 29/4/2020 and 30/4/2020 throughout the watershed  
52  
53  
54  
55  
56  
57  
58  
59  
60

1  
2  
3 might have transported the accumulated contaminants from the impervious surfaces into the river system.  
4  
5 Similar increases in the Ti concentrations <sup>22</sup> and particulate matter associated contaminant (*e.g.*, metals)  
6  
7 concentrations <sup>66,67</sup> with increases in antecedent dry period were observed for road runoff and urban runoff,  
8  
9 respectively.  
10

11  
12 Although we attribute TiO<sub>2</sub> to urban runoff, other sources of TiO<sub>2</sub> engineered particles into surface  
13  
14 waters include recreational activities in the watershed <sup>68</sup>, industrial discharge <sup>23</sup>, or construction activities  
15  
16 <sup>69</sup>, effluents from wastewater treatment plant (WWTP) <sup>70</sup>, and sanitary sewer overflows <sup>20</sup>. The recreational  
17  
18 source (*e.g.*, use of sunscreen during bathing) can be ruled out because there was not any recreational  
19  
20 activities in the three rivers during the sampling period due to ‘coronavirus stay-at-home order’ in South  
21  
22 Carolina <sup>71,72</sup>. The industrial and construction sources also can be ruled out as there was no known industrial  
23  
24 discharge sources and construction activities near the sampling locations which would result in a continuous  
25  
26 discharge of TiO<sub>2</sub> particles to surface water. The human waste source is an insignificant source of TiO<sub>2</sub> to  
27  
28 the river system during the sampling period because of the small size ( $1.1 \pm 0.0$  to  $2.1 \pm 0.1$ ) of the  
29  
30 gadolinium anomaly (**Figure S9**). Gadolinium anomaly is widely used to track effluent from wastewater  
31  
32 treatment plants <sup>73</sup>. Previous studies reported gadolinium anomaly sizes between 1.0 and 30.0 (**Table S9**)  
33  
34 in river streams, and an anomaly > 1.5 has been used as an indicator of wastewater treatment effluent in  
35  
36 rivers. Consequently, the observed TiO<sub>2</sub> engineered particles contamination in this study is attributed to  
37  
38 rainfall events followed by runoff introduction in the rivers, suggesting that the source of TiO<sub>2</sub> particles  
39  
40 here is diffuse urban runoff across the Broad and Congaree Rivers’ watersheds.  
41  
42  
43  
44  
45  
46

## 47 **5. Conclusion**

48  
49  
50 The daily monitoring of the total elemental concentrations, bulk elemental ratios, the number particle  
51  
52 concentration, and the multi-element composition of single particles in the Saluda-Broad-Congaree Rivers’  
53  
54 ecosystem highlights the presence, transient nature, and transport of anthropogenic TiO<sub>2</sub> engineered particle  
55  
56

1  
2  
3 in this urban river ecosystem. The concentration of TiO<sub>2</sub> engineered particle is lowest (0 to 24 μg L<sup>-1</sup>) in  
4  
5 the Lower Saluda River which has the lowest urban footprint. The TiO<sub>2</sub> engineered particle concentrations  
6  
7 increase from the Broad River (0 to 663 μg L<sup>-1</sup>) to the Congaree River (53 to 5050 μg L<sup>-1</sup>) indicating a  
8  
9 continuous and increased introduction of TiO<sub>2</sub> engineered into the Broad and Congaree Rivers with urban  
10  
11 runoff from the urban area of the city of Columbia, South Carolina. Increases in TiO<sub>2</sub> concentrations are  
12  
13 transient and coincident with rainfall with highest concentrations at or near the peak of the discharge. Thus,  
14  
15 the urban environment represents a major source of TiO<sub>2</sub> engineered particle into surface waters. The high  
16  
17 TiO<sub>2</sub> concentrations in the Broad-Congaree Rivers may pose environmental risk in this River ecosystem,  
18  
19 and in other urban rivers, during and following rainfall events, in particular at and near peak discharge.  
20  
21 Higher concentrations of TiO<sub>2</sub> engineered particles, and thus higher environmental risks, can be expected  
22  
23 in more highly urbanized watersheds than the studied urban river ecosystem. The impact of these TiO<sub>2</sub>  
24  
25 engineered particles on river organisms should be further evaluated, including investigating the effect  
26  
27 (bioavailability and toxicity) of TiO<sub>2</sub> engineered particles on several organisms in the trophic chain using  
28  
29 environmentally relevant concentrations, environmentally relevant particle aggregates, and considering  
30  
31 frequent pulse vs. chronic exposure. The design of this study highlights the importance of selecting  
32  
33 sampling sites and monitoring the spatiotemporal variations in engineered particle concentrations in surface  
34  
35 waters for a more comprehensive understanding of the environmental fate, behavior, and risk assessment  
36  
37 of engineered particles. To provide even a more detailed understanding of TiO<sub>2</sub> engineered particle fate and  
38  
39 transport in urban ecosystems, future studies could include additional sampling sites, collect samples at  
40  
41 higher time resolution or over longer sampling periods, collect data following storm events with various  
42  
43 intensities and antecedent dry periods, and collect and analyze sediments samples to determine particle  
44  
45 sedimentation and deposition in the river system.  
46  
47  
48  
49  
50  
51  
52

## 53 **Acknowledgment**

54  
55  
56  
57  
58  
59  
60

1  
2  
3 This work was supported by the US National Science Foundation CAREER (1553909) grant to Dr.  
4  
5 Mohammed Baalousha.  
6  
7  
8  
9

### 10 **Conflict of interest**

11  
12 The authors declare that they have no known competing financial interests or personal relationships  
13  
14 that could have appeared to influence the work reported in this paper.  
15  
16  
17  
18

### 19 **Author contributions**

20  
21 Mr. Nabi and Dr. Wang performed the field work and collected the water samples. Mr. Nabi performed  
22  
23 sample digestion and total metal concentration analysis and wrote the first draft. Dr. Wang performed single  
24  
25 particle analysis. Mr. Erfani and Dr. Goharian developed the clustering analysis code. Dr. Mohammed  
26  
27 Baalousha conceived the overall idea of the research, secured the funding, coordinated the collaboration  
28  
29 among the research team, supervised Mr. Nabi and Dr. Wang in performing experimental work and data  
30  
31 analysis. All authors contributed to the writing and editing of the manuscript.  
32  
33  
34  
35  
36  
37  
38  
39  
40  
41  
42  
43  
44  
45  
46  
47  
48  
49  
50  
51  
52  
53  
54  
55  
56  
57  
58  
59  
60

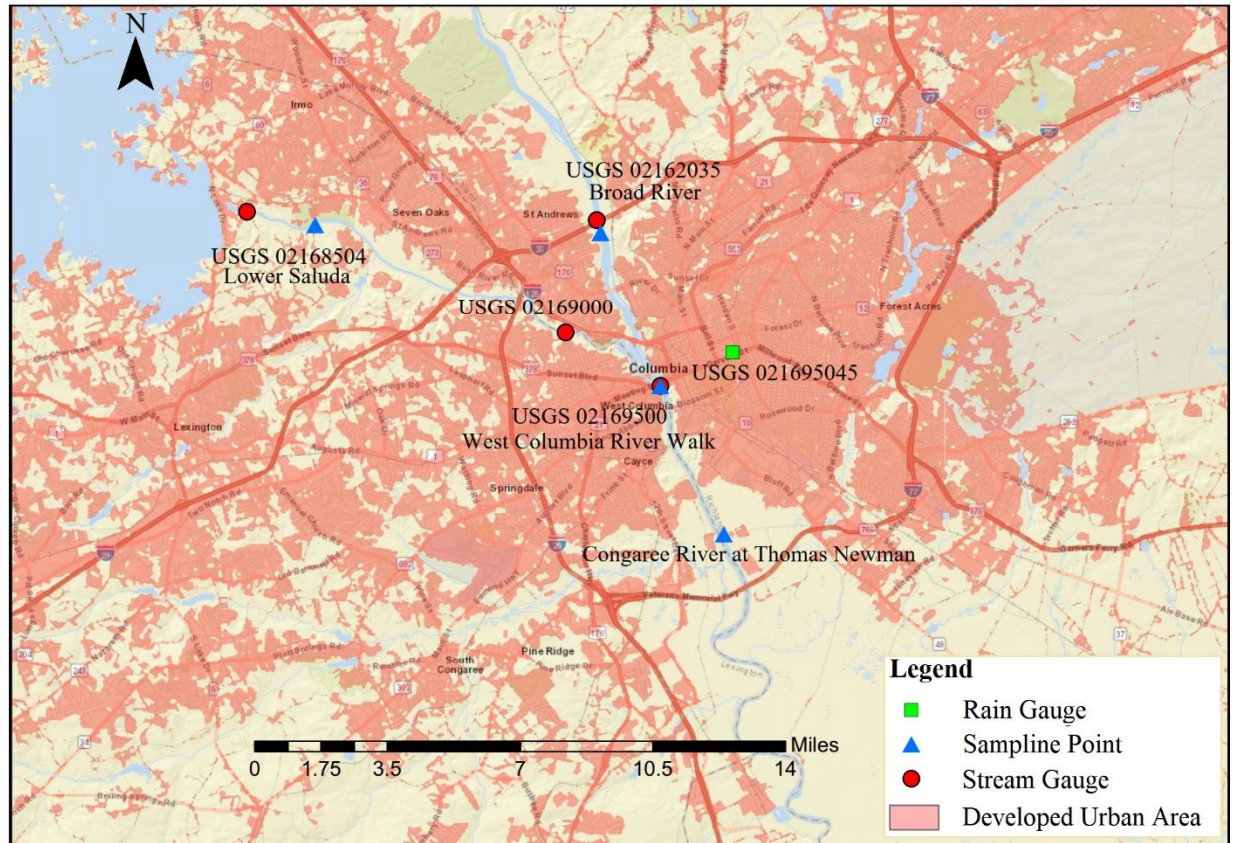


**Figure 1.** Map of the city of Columbia, South Carolina displaying the developed urban area and the sampling locations at the Lower Saluda River (S), Broad River (B), Congaree River at Columbia (Co), and Congaree River at Cayce (C); .



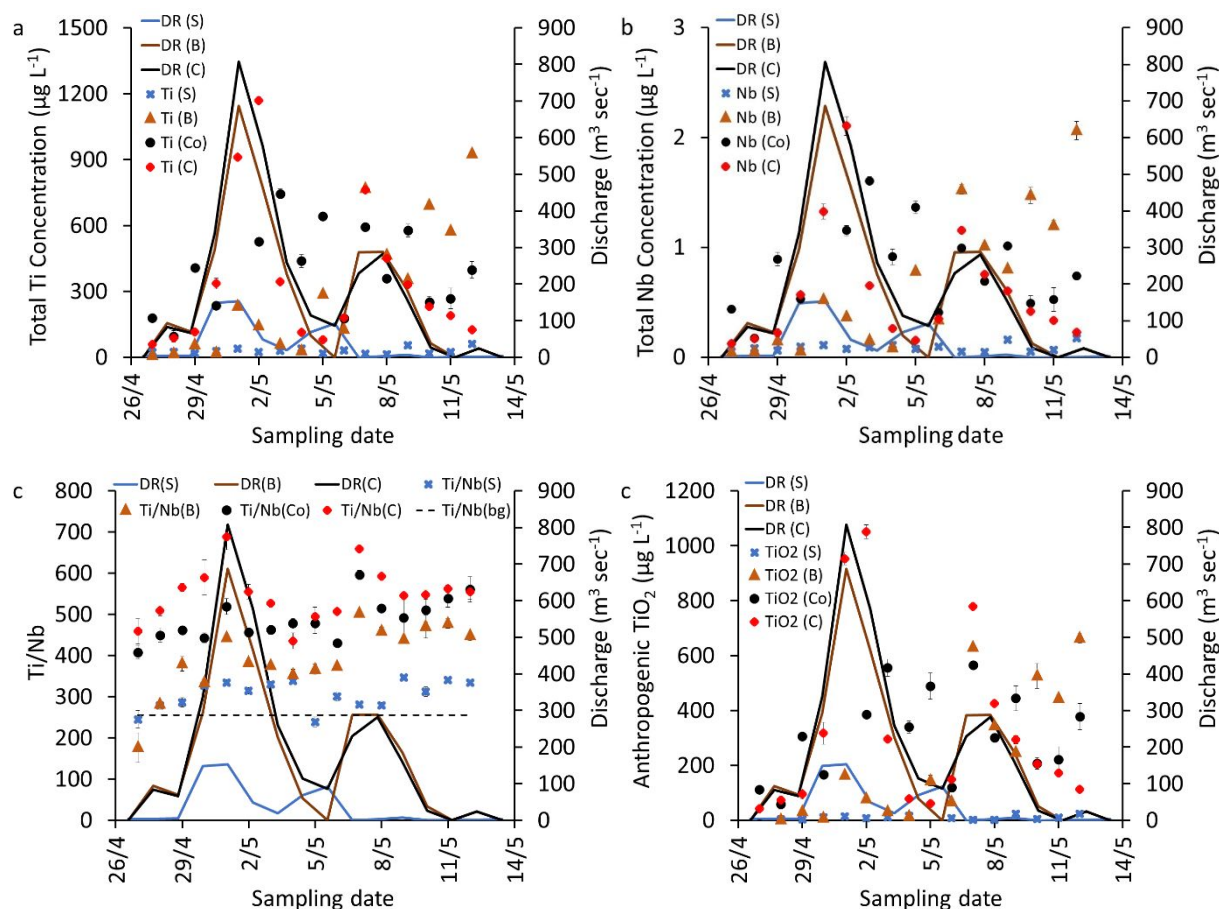


**Figure 2.** Pollutographs of (a and b) the total concentrations of Ti and Nb, (c) Ti/Nb, and (d) the estimated anthropogenic  $\text{TiO}_2$  concentrations in the Lower Saluda River (S), the Broad River (B), and the Congaree River at Columbia (Co) and Cayce (C) during the sampling campaign. DR (S) refers to direct runoff in the Lower Saluda River, DR (B) refers to direct runoff in the Broad River, and DR (Co) refers to direct runoff in the Congaree River at Columbia. The highest Ti, Nb, and  $\text{TiO}_2$  concentrations in the Congaree River at Columbia was  $5976 \pm 89$ ,  $11.5 \pm 0.5$ ,  $5050 \pm 143 \mu\text{g L}^{-1}$  on 1/5/2020 and are not displayed in the Figure.

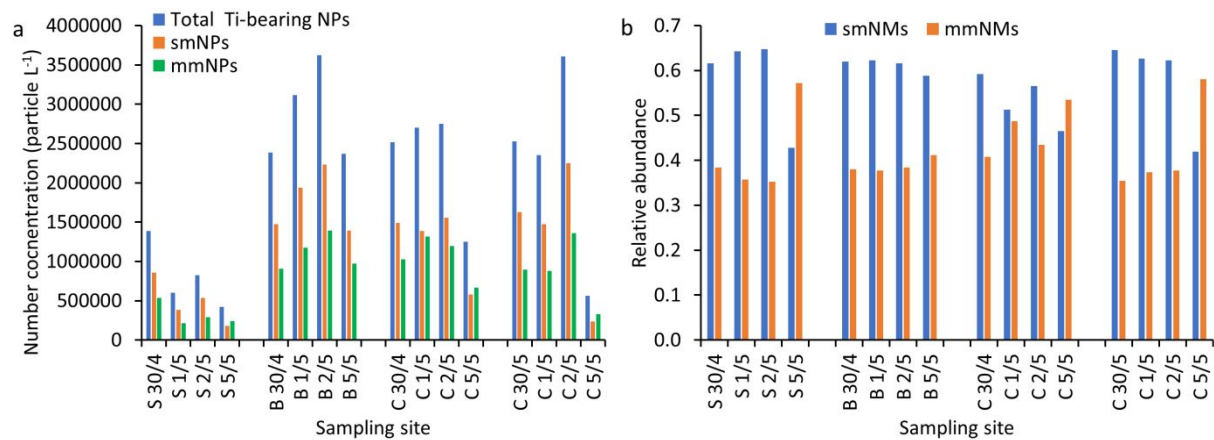


**Figure 3.** (a) Number concentration of total, single metal (sm) and multi-metal (mm), and (b) the relative abundance of sm- and mm- Ti-bearing nanoparticles in the Lower Saluda River (S), Broad River (B), Congaree River at Columbia (Co), and Congaree River at Cayce (C). The number concentrations were corrected by subtracting the number of particles detected in the procedural blanks.

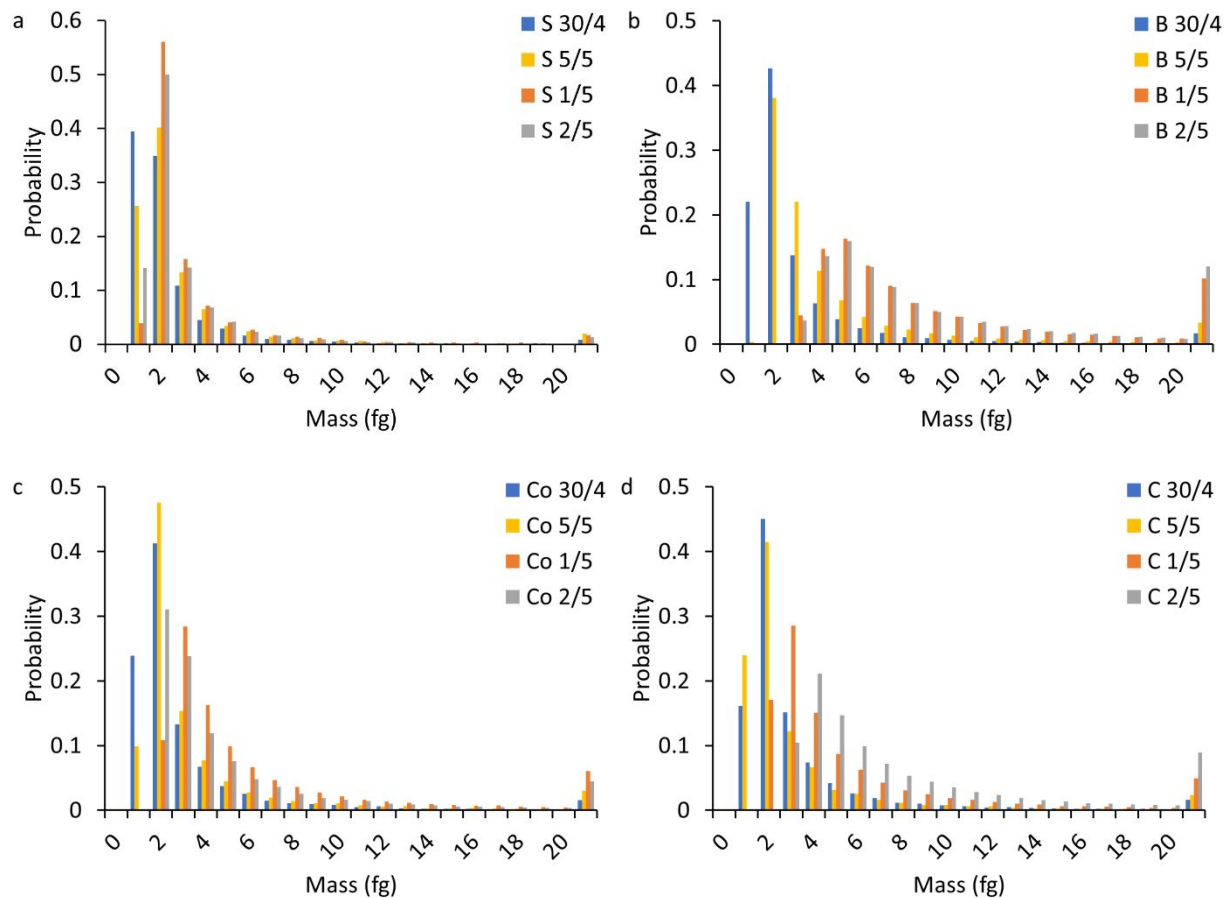


**Figure 4.** Mass distribution of Ti-containing particles in the: (a) Lower Saluda River, (b) Broad River, (c) Congaree River at Columbia, (d) Congaree River at Cayce. S: Lower Saluda River, B: Broad River, Co: Congaree River at Columbia, and C: Congaree River at Cayce.

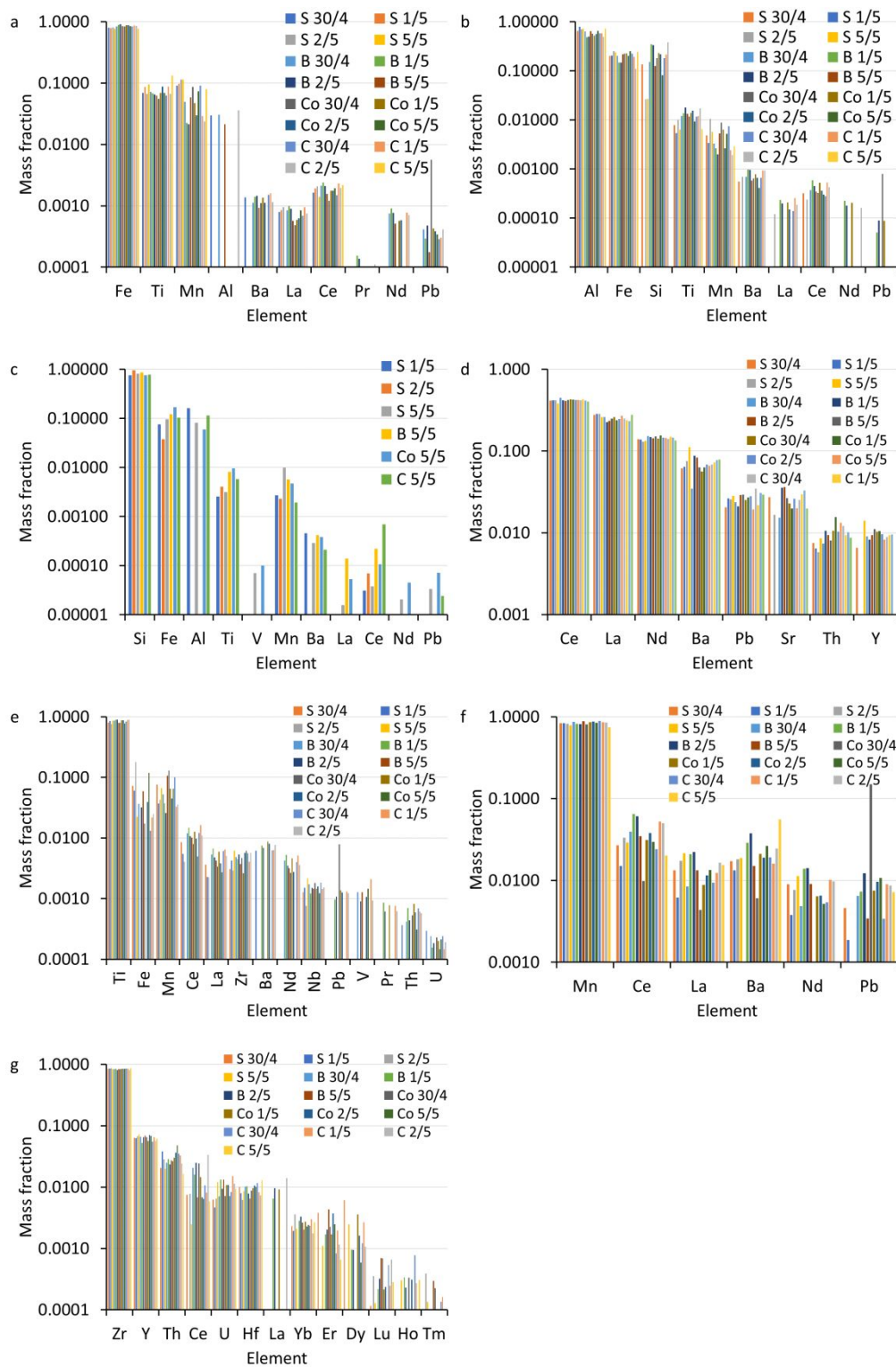


**Figure 5.** Elemental composition of the dominant clusters: (a) Fe-, (b) Al-, (c) Si-, (d) Ce-, (e) Ti-, (f) Mn-, and (g) Zr- rich particle cluster. Standard error was  $<0.05$  for all elements. Note that the Al and Si-rich mmNP clusters are two clusters within the AlSiFe cluster. S: Lower Saluda River, B: Broad River, Co: Congaree River at Columbia, and C: Congaree River at Cayce.

## References:

1. Müller, A., Österlund, H., Marsalek, J. & Viklander, M. The pollution conveyed by urban runoff: A review of sources. *Science of the Total Environment* **709**, 136125 (2020).
2. Kammer, F. von der *et al.* Analysis of engineered nanomaterials in complex matrices (environment and biota): General considerations and conceptual case studies. *Environ. Toxicol. Chem.* **31**, 32–49 (2012).
3. Baalousha, M. *et al.* Outdoor urban nanomaterials: The emergence of a new, integrated, and critical field of study. *Science of the Total Environment* **557–558**, 740–753 (2016).
4. Coatingsworld. Demand for Paint and coatings to reach 1.4 Billion Gallons in 2019 | Statista. (2019). Available at: <https://www.statista.com/statistics/684695/united-states-paint-and-coatings-demand-by-market/>. (Accessed: 22nd April 2020)
5. Göhler, D., Stintz, M., Hillemann, L. & Vorbau, M. Characterization of Nanoparticle Release from Surface Coatings by the Simulation of a Sanding Process. *Ann. Occup. Hyg.* **54**, 615–624 (2010).
6. Koponen, I. K., Jensen, K. A. & Schneider, T. Comparison of dust released from sanding conventional and nanoparticle-doped wall and wood coatings. *J. Expo. Sci. Environ. Epidemiol.* **21**, 408–418 (2011).
7. Nored, A. W., Chalbot, M. C. G. & Kavouras, I. G. Characterization of paint dust aerosol generated from mechanical abrasion of TiO<sub>2</sub>-containing paints. *J. Occup. Environ. Hyg.* **15**, 629–640 (2018).
8. Shandilya, N., Le Bihan, O., Bressot, C. & Morgeneyer, M. Evaluation of the Particle Aerosolization from n-TiO<sub>2</sub> Photocatalytic Nanocoatings under Abrasion. *J. Nanomater.* **2014**, 185080 (2014).

- 1  
2  
3 9. Shandilya, N., Le Bihan, O. & Morgeneyer, M. A Review on the Study of the Generation of  
4 (Nano)particles Aerosols during the Mechanical Solicitation of Materials. *J. Nanomater.* **2014**,  
5 (2014).  
6  
7  
8  
9
- 10 10. Tou, F. *et al.* Multi method approach for analysis of road dust particles: elemental ratios, SP-ICP-  
11 TOF-MS, and TEM. *ESNano (2022, Rev.*  
12  
13
- 14 11. Thorpe, A. & Harrison, R. M. Sources and properties of non-exhaust particulate matter from road  
15 traffic: A review. *Sci. Total Environ.* **400**, 270–282 (2008).  
16  
17  
18
- 19 12. Gietl, J. K., Lawrence, R., Thorpe, A. J. & Harrison, R. M. Identification of brake wear particles  
20 and derivation of a quantitative tracer for brake dust at a major road. *Atmos. Environ.* **44**, 141–146  
21 (2010).  
22  
23  
24  
25
- 26 13. Wåhlin, P., Berkowicz, R. & Palmgren, F. Characterisation of traffic-generated particulate matter  
27 in Copenhagen. *Atmos. Environ.* **40**, 2151–2159 (2006).  
28  
29  
30
- 31 14. Apeagyei, E., Bank, M. S. & Spengler, J. D. Distribution of heavy metals in road dust along an  
32 urban-rural gradient in Massachusetts. *Atmos. Environ.* **45**, 2310–2323 (2011).  
33  
34  
35
- 36 15. Pant, P. & Harrison, R. M. Estimation of the contribution of road traffic emissions to particulate  
37 matter concentrations from field measurements: A review. *Atmos. Environ.* **77**, 78–97 (2013).  
38  
39  
40
- 41 16. Adachi, K. & Tainosho, Y. Characterization of heavy metal particles embedded in tire dust.  
42 *Environ. Int.* **30**, 1009–1017 (2004).  
43  
44  
45
- 46 17. Wang, J. *et al.* Detection and quantification of engineered particles in urban runoff. *Chemosphere*  
47 **248**, 126070 (2020).  
48  
49  
50
- 51 18. USGS. *Characterization of Stormwater Runoff from Bridges in North Carolina and the Effects of*  
52 *Bridge Deck Runoff on Receiving Streams.* (2011).  
53  
54  
55  
56

- 1  
2  
3 19. Bourcier, D. R., Hindin, E. & Cook, J. C. Titanium and tungsten in highway runoff at pullman,  
4 washington. *Int. J. Environ. Stud.* **15**, 145–149 (1980).  
5  
6  
7  
8 20. Loosli, F. *et al.* Sewage spills are a major source of titanium dioxide engineered (nano)-particle  
9 release into the environment. *Environ. Sci. Nano* **6**, 763–777 (2019).  
10  
11  
12  
13 21. Saharia, A. M., Zhu, Z., Aich, N., Baalousha, M. & Atkinson, J. F. Modeling the transport of  
14 titanium dioxide nanomaterials from combined sewer overflows in an urban river. *Sci. Total*  
15 *Environ.* **696**, 133904 (2019).  
16  
17  
18  
19  
20 22. Nabi, M. M., Wang, J. & Baalousha, M. Episodic surges in titanium dioxide engineered particle  
21 concentrations in surface waters following rainfall events. *Chemosphere* **263**, 128261 (2021).  
22  
23  
24  
25 23. Slomberg, D. L. *et al.* Anthropogenic Release and Distribution of Titanium Dioxide Particles in a  
26 River Downstream of a Nanomaterial Manufacturer Industrial Site. *Front. Environ. Sci.* **0**, 76  
27 (2020).  
28  
29  
30  
31  
32 24. Vidmar, J., Zuliani, T., Milačič, R. & Ščančar, J. Following the Occurrence and Origin of  
33 Titanium Dioxide Nanoparticles in the Sava River by Single Particle ICP-MS. *Water* **14**, 959  
34 (2022).  
35  
36  
37  
38  
39 25. Parker, N. & Keller, A. A. Variation in regional risk of engineered nanoparticles: nanoTiO<sub>2</sub> as a  
40 case study. *Environ. Sci. Nano* **6**, 444–455 (2019).  
41  
42  
43  
44 26. Rand, L. N. *et al.* Quantifying temporal and geographic variation in sunscreen and mineralogic  
45 titanium-containing nanoparticles in three recreational rivers. *Sci. Total Environ.* **743**, 140845  
46 (2020).  
47  
48  
49  
50  
51 27. Gondikas, A. P. *et al.* Release of TiO<sub>2</sub> nanoparticles from sunscreens into surface waters: A one-  
52 year survey at the old danube recreational lake. *Environ. Sci. Technol.* **48**, 5415–5422 (2014).  
53  
54  
55  
56 28. David Holbrook, R. *et al.* Titanium distribution in swimming pool water is dominated by dissolved  
57  
58  
59  
60

- 1  
2  
3 species. *Environ. Pollut.* **181**, 68–74 (2013).  
4  
5  
6 29. Yang, Y. *et al.* Prospecting nanomaterials in aqueous environments by cloud-point extraction  
7 coupled with transmission electron microscopy. *Sci. Total Environ.* **584–585**, 515–522 (2017).  
8  
9  
10 30. Venkatesan, A. K. *et al.* Detection and Sizing of Ti-Containing Particles in Recreational Waters  
11 Using Single Particle ICP-MS. *Bull. Environ. Contam. Toxicol.* **100**, 120–126 (2018).  
12  
13  
14  
15 31. Praetorius, A. *et al.* Single-particle multi-element fingerprinting (spMEF) using inductively-  
16 coupled plasma time-of-flight mass spectrometry (ICP-TOFMS) to identify engineered  
17 nanoparticles against the elevated natural background in soils. *Environ. Sci. Nano* **4**, 307–314  
18 (2017).  
19  
20  
21  
22  
23  
24 32. Wang, H., Adeleye, A. S., Huang, Y., Li, F. & Keller, A. A. Heteroaggregation of nanoparticles  
25 with biocolloids and geocolloids. *Adv. Colloid Interface Sci.* **226**, 24–36 (2015).  
26  
27  
28  
29 33. Barksdale, J. Titanium, Its Occurrence, Chemistry, and Technology : Soil Science. in 414 (1950).  
30  
31  
32 34. Zack, T., Kronz, A., Foley, S. . & Rivers, T. Trace element abundances in rutiles from eclogites  
33 and associated garnet mica schists. *Chem. Geol.* **184**, 97–122 (2002).  
34  
35  
36  
37 35. Craigie, N. *Principles of Elemental Chemostratigraphy*. Springer International Publishing  
38 (Springer International Publishing, 2018). doi:10.1007/978-3-319-71216-1  
39  
40  
41  
42 36. Wang, J., Nabi, M.M., Mahdi, E, Goharian, E, Baalousha, M. Identification and Quantification of  
43 Anthropogenic Nanomaterials in Urban Rainfall and Runoff Using Single Particle-Inductively  
44 Coupled Plasma-Time of Flight-Mass Spectrometry (In preparation).  
45  
46  
47  
48  
49 37. Nabi, M. M. *et al.* Concentrations and size distribution of TiO<sub>2</sub> and Ag engineered particles in five  
50 wastewater treatment plants in the United States. *Sci. Total Environ.* **753**, 142017 (2021).  
51  
52  
53  
54 38. Praetorius, A. *et al.* Single-particle multi-element fingerprinting (spMEF) using inductively-  
55  
56  
57  
58  
59  
60



- 1  
2  
3 coupled plasma time-of-flight mass spectrometry (ICP-TOFMS) to identify engineered  
4 nanoparticles against the elevated natural background in soils. *Environ. Sci. Nano* **4**, 307–314  
5 (2017).  
6  
7  
8  
9
- 10 39. Lee, S. *et al.* Nanoparticle size detection limits by single particle ICP-MS for 40 elements.  
11 *Environ. Sci. Technol.* **48**, 10291–10300 (2014).  
12  
13
- 14 40. Hadioui, M. *et al.* Lowering the Size Detection Limits of Ag and TiO<sub>2</sub> Nanoparticles by Single  
15 Particle ICP-MS. *Anal. Chem.* **91**, 13275–13284 (2019).  
16  
17  
18
- 19 41. Pace, H. E. *et al.* Determining Transport Efficiency for the Purpose of Counting and Sizing  
20 Nanoparticles via Single Particle Inductively Coupled Plasma Mass Spectrometry. *Anal. Chem.*  
21 **83**, 9361–9369 (2011).  
22  
23  
24  
25
- 26 42. Baalousha, M., Wang, J., Erfani, M. & Goharian, E. Elemental fingerprints in natural  
27 nanomaterials determined using SP-ICP-TOF-MS and clustering analysis. *Sci. Total Environ.* **792**,  
28 148426 (2021).  
29  
30  
31  
32  
33
- 34 43. Antignano, A. & Manning, C. E. Rutile solubility in H<sub>2</sub>O, H<sub>2</sub>O–SiO<sub>2</sub>, and H<sub>2</sub>O–NaAlSi<sub>3</sub>O<sub>8</sub>  
35 fluids at 0.7–2.0 GPa and 700–1000 °C: Implications for mobility of nominally insoluble  
36 elements. *Chem. Geol.* **255**, 283–293 (2008).  
37  
38  
39  
40
- 41 44. U.S. Geological Survey. *Mineral Commodity Summaries. Mineral Commodity Summaries* (2019).  
42 doi:10.3133/70202434  
43  
44
- 45 45. U.S. Geological Survey (USGS). USGS Current Conditions for USGS 03451500 FRENCH  
46 BROAD RIVER AT ASHEVILLE, NC. Available at:  
47 [https://waterdata.usgs.gov/nwis/dv?cb\\_00045=on&format=html&site\\_no=03451500&referred\\_molecule=sw&period=&begin\\_date=2020-04-20&end\\_date=2020-05-10](https://waterdata.usgs.gov/nwis/dv?cb_00045=on&format=html&site_no=03451500&referred_molecule=sw&period=&begin_date=2020-04-20&end_date=2020-05-10). (Accessed: 8th January  
48  
49  
50  
51  
52  
53  
54  
55  
56  
57  
58  
59  
60

- 1  
2  
3 46. City of Knoxville. Rainfall Data - City of Knoxville. Available at:  
4  
5 [https://knoxvilletn.gov/government/city\\_departments\\_offices/engineering/stormwater\\_engineering](https://knoxvilletn.gov/government/city_departments_offices/engineering/stormwater_engineering)  
6  
7 [\\_division/rainfall\\_data](https://knoxvilletn.gov/government/city_departments_offices/engineering/stormwater_engineering). (Accessed: 8th January 2021)  
8  
9
- 10 47. U.S. Geological Survey (USGS). USGS Current Conditions for USGS 02162285 TABLE ROCK  
11 RESERVOIR NR CLEVELAND, SC. Available at:  
12  
13 [https://waterdata.usgs.gov/nwis/dv?cb\\_00045=on&format=html&site\\_no=02162285&referred\\_mo](https://waterdata.usgs.gov/nwis/dv?cb_00045=on&format=html&site_no=02162285&referred_mo)  
14  
15 [dule=sw&period=&begin\\_date=2020-04-27&end\\_date=2020-05-12](https://waterdata.usgs.gov/nwis/dv?cb_00045=on&format=html&site_no=02162285&referred_mo). (Accessed: 10th January  
16  
17 2021)  
18  
19
- 20  
21 48. SCDHEC. Saluda River/Lake Murray watershed. Available at:  
22  
23 <https://scdhec.gov/sites/default/files/docs/HomeAndEnvironment/Docs/03050109-13.pdf>.  
24  
25 (Accessed: 16th August 2021)  
26  
27
- 28 49. SCE & G, S. C. *Saluda Project (FERC No. 516): Lake Murray Water Quality Report*.  
29  
30
- 31 50. National Park Service & U.S. Department of the Interior. *Assessment of Water Resources and*  
32  
33 *Watershed Conditions in Congaree National Park, South Carolina*. (2010).  
34  
35
- 36 51. Federal Energy Regulatory Commission. ENVIRONMENTAL ASSESSMENT FOR  
37  
38 HYDROPOWER LICENSE. (2020).  
39  
40
- 41 52. SCE & G, S. C. *South Carolina Electric & Gas COL Application Part 3-Environmental Report*.  
42  
43
- 44 53. Galfi, H., Österlund, H., Marsalek, J. & Viklander, M. Mineral and Anthropogenic Indicator  
45  
46 Inorganics in Urban Stormwater and Snowmelt Runoff: Sources and Mobility Patterns. *Water. Air.*  
47  
48 *Soil Pollut.* **228**, 1–18 (2017).  
49  
50
- 51 54. Wu, J. *et al.* Metal-Containing Nanoparticles in Low-Rank Coal-Derived Fly Ash from China:  
52  
53 Characterization and Implications toward Human Lung Toxicity. *Environ. Sci. Technol.* **55**, 6644–  
54  
55 6654 (2021).  
56  
57  
58  
59  
60

- 1  
2  
3 55. Gondikas, A. *et al.* Where is the nano? Analytical approaches for the detection and quantification  
4 of TiO<sub>2</sub> engineered nanoparticles in surface waters. *Environ. Sci. Nano* **5**, 313–326 (2018).  
5  
6  
7  
8 56. Markus, A. A. *et al.* Determination of metal-based nanoparticles in the river Dommel in the  
9 Netherlands via ultrafiltration, HR-ICP-MS and SEM. *Sci. Total Environ.* **631–632**, 485–495  
10 (2018).  
11  
12  
13  
14  
15 57. Kaegi, R. *et al.* Synthetic TiO<sub>2</sub> nanoparticle emission from exterior facades into the aquatic  
16 environment. *Environ. Pollut.* **156**, 233–239 (2008).  
17  
18  
19  
20 58. Adamiec, E. Road environments: Impact of metals on human health in heavily congested cities of  
21 Poland. *Int. J. Environ. Res. Public Health* **14**, (2017).  
22  
23  
24  
25 59. Pereira, E., Baptista-Neto, J. A., Smith, B. J. & McAllister, J. J. The contribution of heavy metal  
26 pollution derived from highway runoff to Guanabara Bay sediments - Rio de Janeiro / Brazil. *An.*  
27 *Acad. Bras. Cienc.* **79**, 739–750 (2007).  
28  
29  
30  
31  
32 60. Chemours. Ti-Pure™ Solutions for Coatings: Applications. (2018). Available at:  
33 [https://www.tipure.com/en/applications/coatings?\\_ga=2.22333115.1280235886.1586571265-](https://www.tipure.com/en/applications/coatings?_ga=2.22333115.1280235886.1586571265-1482119140.1586571265)  
34 [1482119140.1586571265](https://www.tipure.com/en/applications/coatings?_ga=2.22333115.1280235886.1586571265-1482119140.1586571265). (Accessed: 10th April 2020)  
35  
36  
37  
38  
39 61. Shandilya, N., Le Bihan, O., Bressot, C. & Morgeneyer, M. Emission of titanium dioxide  
40 nanoparticles from building materials to the environment by wear and weather. *Environ. Sci.*  
41 *Technol.* **49**, 2163–2170 (2015).  
42  
43  
44  
45  
46 62. Lee, P. K. *et al.* Lead chromate detected as a source of atmospheric Pb and Cr (VI) pollution. *Sci.*  
47 *Rep.* **6**, 1–10 (2016).  
48  
49  
50  
51 63. Wilczyńska-Michalik, W., Rzeźnikiewicz, K., Pietras, B. & Michalik, M. Fine and ultrafine TiO<sub>2</sub>  
52 particles in aerosol in Kraków (Poland). *Mineralogia* **45**, 65–77 (2014).  
53  
54  
55  
56 64. Survey, U. S. G. *Mineral Commodity Summaries. Mineral Commodity Summaries* (2019).  
57  
58  
59  
60

- 1  
2  
3 doi:10.3133/70202434  
4  
5  
6 65. Wang, J., Nabi, M. M., Erfani, M., Goharian, E. & Baalousha, M. Identification and quantification  
7 of anthropogenic nanomaterials in urban rain and runoff using single particle-inductively coupled  
8 plasma-time of flight-mass spectrometry. *Environ. Sci. Nano* **9**, 714–729 (2022).  
9  
10  
11  
12 66. Tian, P., Li, Y. & Yang, Z. Effect of rainfall and antecedent dry periods on heavy metal loading of  
13 sediments on urban roads. *Front. Earth Sci. China* **3**, 297–302 (2009).  
14  
15  
16  
17 67. Yuan, Q., Guerra, H. & Kim, Y. An Investigation of the Relationships between Rainfall  
18 Conditions and Pollutant Wash-Off from the Paved Road. *Water* **9**, 232 (2017).  
19  
20  
21  
22 68. Reed, R. B. *et al.* Multi-day diurnal measurements of Ti-containing nanoparticle and organic  
23 sunscreen chemical release during recreational use of a natural surface water. *Environ. Sci. Nano*  
24 **4**, 69–77 (2017).  
25  
26  
27  
28  
29 69. Kaegi, R. *et al.* Release of TiO<sub>2</sub> – (Nano) particles from construction and demolition landfills.  
30 *NanoImpact* **8**, 73–79 (2017).  
31  
32  
33  
34 70. Kiser, M. A. *et al.* Titanium nanomaterial removal and release from wastewater treatment plants.  
35 *Environ. Sci. Technol.* **43**, 6757–6763 (2009).  
36  
37  
38  
39 71. City of West Columbia City Council. West Columbia City Operated Parks Closed to Reduce  
40 Potential COVID-19 Exposure - City of West Columbia. Available at:  
41 [https://westcolumbiasc.gov/2020/03/west-columbia-city-operated-parks-closed-to-reduce-](https://westcolumbiasc.gov/2020/03/west-columbia-city-operated-parks-closed-to-reduce-potential-covid-19-exposure/)  
42 [potential-covid-19-exposure/](https://westcolumbiasc.gov/2020/03/west-columbia-city-operated-parks-closed-to-reduce-potential-covid-19-exposure/). (Accessed: 8th January 2021)  
43  
44  
45  
46  
47  
48 72. City of Columbia. City of Columbia coronavirus (COVID-19) update - Stay at Home Order issued  
49 - Tuesday, March 24 at 10 a.m. Available at:  
50 <https://www.como.gov/CMS/pressreleases/view.php?id=6656>. (Accessed: 8th January 2021)  
51  
52  
53  
54  
55 73. Verplanck, P. L. *et al.* Evaluating the behavior of gadolinium and other rare earth elements  
56  
57  
58  
59  
60

- 1  
2  
3 through large metropolitan sewage treatment plants. *Environ. Sci. Technol.* **44**, 3876–3882 (2010).  
4  
5  
6 74. U.S. Army Corps of Engineers & Stanley Consultants. *Saluda River Basin, Charleston district*  
7 *navigability study*. (1977).  
8  
9  
10 75. Congaree River Keeper. Lower Saluda River. Available at:  
11 <https://www.congareeriverkeeper.org/lower-saluda-river>. (Accessed: 8th January 2021)  
12  
13  
14 76. SCDHEC. *Watershed Water Quality Assessment Saluda River Basin*. (2011).  
15  
16  
17 77. SCDOT. Annual average daily traffic. (2019). Available at:  
18 <https://www.scdot.org/travel/pdf/trafficcounts/2019/Lexington.pdf>. (Accessed: 2nd April 2021)  
19  
20  
21 78. SCDOT. Annual average daily traffic. (2019). Available at:  
22 <https://www.scdot.org/travel/pdf/trafficcounts/2019/Richland.pdf>. (Accessed: 1st April 2021)  
23  
24  
25 79. NC DEQ. *Broad river Basin restoration priorities*. (2009).  
26  
27  
28  
29  
30 80. Jochum, K. P. *et al.* Reference Values Following ISO Guidelines for Frequently Requested Rock  
31 Reference Materials. *Geostand. Geoanalytical Res.* **40**, 333–350 (2016).  
32  
33  
34 81. Kulaksiz, S. & Bau, M. Contrasting behaviour of anthropogenic gadolinium and natural rare earth  
35 elements in estuaries and the gadolinium input into the North Sea. *Earth Planet. Sci. Lett.* **260**,  
36 361–371 (2007).  
37  
38  
39 82. Bau, M., Knappe, A. & Dulski, P. Anthropogenic gadolinium as a micropollutant in river waters in  
40 Pennsylvania and in Lake Erie, northeastern United States. *Chemie der Erde* **66**, 143–152 (2006).  
41  
42  
43 83. Kulaksiz, S. & Bau, M. Rare earth elements in the Rhine River, Germany: First case of  
44 anthropogenic lanthanum as a dissolved microcontaminant in the hydrosphere. *Environ. Int.* **37**,  
45 973–979 (2011).  
46  
47  
48 84. Bau, M. & Dulski, P. Anthropogenic origin of positive gadolinium anomalies in river waters.  
49  
50  
51  
52  
53  
54  
55  
56  
57  
58  
59  
60

- 1  
2  
3 *Earth Planet. Sci. Lett.* **143**, 245–255 (1996).  
4  
5  
6 85. Knappe, A., Möller, P., Dulski, P. & Pekdeger, A. Positive gadolinium anomaly in surface water  
7 and ground water of the urban area Berlin, Germany. *Geochemistry* **65**, 167–189 (2005).  
8  
9  
10 86. Elbaz-Poulichet, F., Seidel, J. L. & Othoniel, C. Occurrence of an anthropogenic gadolinium  
11 anomaly in river and coastal waters of Southern France. *Water Res.* **36**, 1102–1105 (2002).  
12  
13  
14  
15 87. Möller, P., Paces, T., Dulski, P. & Morteani, G. Anthropogenic Gd in surface water, drainage  
16 system, and the water supply of the City of Prague, Czech Republic. *Environ. Sci. Technol.* **36**,  
17 2387–2394 (2002).  
18  
19  
20  
21  
22 88. Nozaki, Y., Lerche, D., Alibo, D. S. & Tsutsumi, M. Dissolved indium and rare earth elements in  
23 three Japanese rivers and Tokyo Bay: Evidence for anthropogenic Gd and In. *Geochim.*  
24 *Cosmochim. Acta* **64**, 3975–3982 (2000).  
25  
26  
27  
28  
29 89. Hissler, C., Stille, P., Guignard, C., François Iffly, J. & Pfister, L. Rare Earth Elements as  
30 hydrological tracers of anthropogenic and critical zone contributions: a case study at the Alzette  
31 River basin scale. *Procedia Earth Planet. Sci.* **10**, 349–352 (2014).  
32  
33  
34  
35  
36  
37  
38  
39  
40  
41  
42  
43  
44  
45  
46  
47  
48  
49  
50  
51  
52  
53  
54  
55  
56  
57  
58  
59  
60